ALEPH 97-035
PHYSIC 97-030
S. Wasserbaech
1 April 1997

Measurement of the τ lifetime with the IPD method: 1993 and 1994 data

Steve Wasserbaech, University of Washington

Abstract

The impact parameter difference method is used to measure the mean lifetime of the τ lepton from the 1993 and 1994 ALEPH data samples. The procedures are modified slightly with respect to the published 1992 analysis. The lifetime measured from the 1993 and 1994 data is $\tau_\tau = 290.4 \pm 3.2 \pm 1.3$ fs.

1 Introduction

The impact parameter difference (IPD) method was described in previous notes [1–3]. The published ALEPH IPD results [4–6] are $\tau_\tau = 285 \pm 17 \pm 6$ fs (1989+90 data), $310.5 \pm 13.0 \pm 3.5$ fs (1991), and $288.4 \pm 5.6 \pm 1.4$ fs (1992). The soon-to-be-published ALEPH result combining all methods and all years analyzed so far is $\tau_\tau = 291.2 \pm 2.0 \pm 1.2$ fs [7].

In this memo I describe the IPD analysis of the ALEPH data collected in 1993 and 1994. The analysis is very similar to that described in [3]; the few minor improvements that have been made are explained below.

The IPD method is applied to events of 1-1 topology. For each event we measure d_0 and ϕ_0 of the + and − daughter tracks. The production angle θ of the τ pair is estimated from the event thrust axis, determined from the `enflw` objects. For each event I compute

$$Y = d_+ - d_- \tag{1}$$

and

$$X = \frac{\bar{p}_\tau(\sqrt{s})}{\bar{p}^0_\tau} \Delta\phi \, \sin\theta, \tag{2}$$

where $\Delta\phi = \phi_+ - \phi_- \pm \pi$, $\bar{p}_\tau(\sqrt{s})$ is the average τ momentum, calculated from Monte Carlo after the event selection criteria are applied, and $\bar{p}_\tau^0 = \bar{p}_\tau(91.25\,\mathrm{GeV})$. For a particular value of X, the mean value of Y is given by

$$\langle Y \rangle = \left[\frac{\bar{p}_\tau^0}{M_\tau} \tau_\tau \right] X. \tag{3}$$

The quantity in brackets corresponds to the slope of $\langle Y \rangle$ vs. X and is equal to the mean τ laboratory decay length at the peak. The mean decay length is extracted from the Y vs. X distribution by means of an unbinned, weighted, least-squares fit and an iterative trimming procedure for removing poorly measured events. The fitting function is

$$\langle Y \rangle = a_0 + a_1 X. \tag{4}$$

In practice, the fitted slope a_1 is related to the mean τ lifetime by

$$a_1 = \frac{\bar{p}_\tau^0}{M_\tau}(1 + D)\tau_\tau, \tag{5}$$

where D characterizes the systematic biases inherent in the method or related to measurement errors.

2 Data Sample

The run selection is based on the intersection of the official "Physics Groups" selections "VDET," "Heavy Flavor ECAL," and "Heavy Flavor HCAL" (from `scanbook`). The `run_qual` reports are also studied and some runs with potentially serious problems for the lifetime measurement are removed. Table 1 contains some details about the resulting τ lifetime data samples. The combined 1993 and 1994 sample contains 1.146×10^5 produced $\tau^+\tau^-$ events and corresponds to 2.36 million produced $q\bar{q}$ events or $87.64\,\mathrm{pb}^{-1}$.

Table 1. Statistics in the 1993 and 1994 τ lifetime data samples. The data in the last two columns are derived from the observed numbers of $q\bar{q}$ (class 16) events passing `xlumok`, the hadronic cross sections measured by ALEPH, and the $\tau^+\tau^-$ cross sections predicted by `korl07`.

Year	Energy	Runs	Mean $\sqrt{s}$ (GeV)	`xlumok` Cl 16 events	Integrated lumi (pb^{-1})	Produced $\tau^+\tau^-$
1993	-2	242	89.428	80492	8.24	4000
	peak	756	91.226	445948	14.97	22100
	$+2$	251	93.013	116860	8.47	5800
	total	1249	91.325	643300	31.69	31900
1994	peak	2574	91.201	1666234	55.95	82700

3 Monte Carlo

The $\tau^+\tau^-$ Monte Carlo used in this analysis was generated with `korl07`. `galeph` 256.2 and 303 were used for the 1993 and 1994 samples, respectively; the corresponding `julia` version numbers were 276.4 and 278. The 1993 $\tau^+\tau^-$ sample, consisting of 415K generated events, has the correct proportions of peak and off-peak events. The 1994 $\tau^+\tau^-$ sample contains 455K events. The generated τ mass and lifetime are 1776.9 MeV/c^2 and 296 fs.

The small effect of backgrounds on the lifetime measurement is studied using Monte Carlo samples of $e^+e^- \to e^+e^-$ (`unibab`), $e^+e^- \to \mu^+\mu^-$, $e^+e^- \to q\bar{q}$, $\gamma\gamma \to \ell^+\ell^-$, and $\gamma\gamma \to q\bar{q}$. The W cutoff for two-photon final states is set to 2 GeV/c^2 in `phot02`. The dominant source of background in the 1-1 sample is $\gamma\gamma \to \ell^+\ell^-$ events, amounting to only 0.24% at the peak. (See section 12.9.) The Monte Carlo sample sizes are listed in table 2.

4 Beam position and size

Throughout this analysis, track impact parameters are measured with respect to the chunk-by-chunk `qfget_bp` beam axis positions. In the real data, selected tracks from chunks of roughly 75 Z^0 events are used to determine the x and y coordinates of the beam axis with uncertainties of approximately 20 and 10 μm, respectively. Tracks from τ pair events are not used.

The horizontal size of the luminous region, σ_x, is measured by means of a technique, based on `qfndip`, developed by Brown and Gay. For these measurements the data is divided into "metachunks" of roughly 275 $q\bar{q}$ events. The resolution is given by $\Delta\sigma_x = 0.539(\sigma_x \oplus 105\,\mu\text{m})/\sqrt{N}$, where N is the number of $q\bar{q}$ events in the metachunk. The σ_x values are accessed by means of the `alpha` routine `qbeamx` and are used in the calculation of the event weights in the fit for the mean τ decay length. The average values of σ_x are 159 μm in 1993 and 125 μm in 1994. Figure 1 shows the σ_x distributions for the

Table 2. Statistics in the Monte Carlo samples used in the analysis. The sizes of the samples are expressed in units of the real data sample size in each year.

	MC sample size	
Reaction	1993	1994
$e^+e^- \to \tau^+\tau^-$	13	5.5
$e^+e^- \to e^+e^-$	1	3
$e^+e^- \to \mu^+\mu^-$	3	3
$e^+e^- \to q\bar{q}$	1	1
$\gamma\gamma \to e^+e^-$	1	3
$\gamma\gamma \to \mu^+\mu^-$	3	3
$\gamma\gamma \to \tau^+\tau^-$	3	3
$\gamma\gamma \to q\bar{q}$	1	1

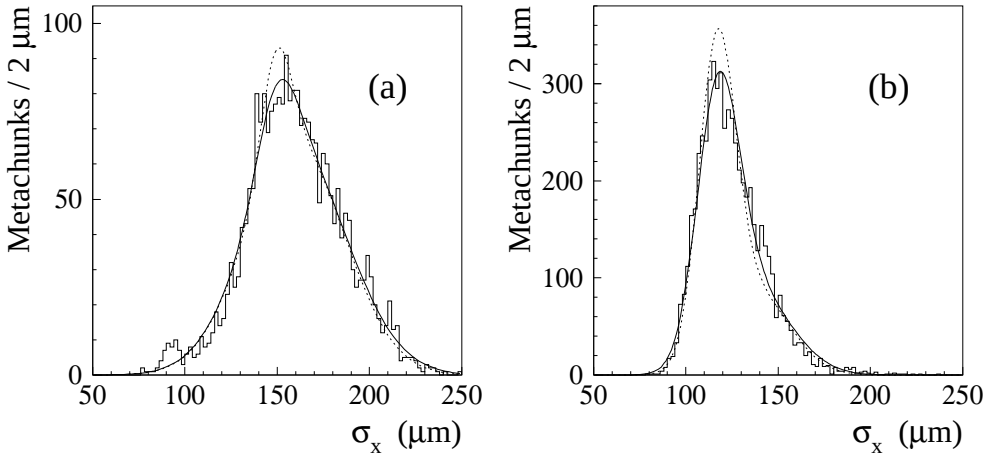

Figure 1. σ_x distributions for (a) 1993 and (b) 1994. The histograms show the measured σ_x distributions in the metachunks (VDET run selection). In each year, the true distribution of σ_x is assumed to be the sum of two Gaussians. The solid curves represent the best fit to the measured distributions; the dotted curves show the corresponding true distributions of σ_x.

metachunks of 1993 and 1994. For analysis of Monte Carlo events, `qfget_bp` and `qbeamx` simulate the appropriate distribution of σ_x, as well as the uncertainties on the beam position and on σ_x as in the real data.

5 Exclusion zones

Two potentially serious detector problems were present for extended periods in 1993 and 1994. It was decided to handle these problems by excluding regions of θ and ϕ during those periods, rather than by killing the runs entirely.

First, swapped cables in ECAL Endcap A during runs 22793–22880 (1993) could lead to increased Bhabha background, so events in which either daughter track has $\cos\theta > 0.72$ are removed during this period. Since the overlap of the ECAL endcap and VDET is small, the loss of statistics is only 0.6% of the 1993 τ lifetime sample.

Second, there were problems with the gating in some sectors of TPC End B during the first part of 1994 (run < 26330, corresponding to 9.4% of the integrated luminosity of 1994). Although the d_0 resolution has been recovered to a large extent by means of time-dependent field corrections in `julia`, the corrections are rather large and I prefer to remove events that involve the affected parts of the detector. The generously chosen exclusion zone is $-183° < \phi < 23°$ in End B, removing 5.4% of the events in the 1994 sample. This cut violates the 2π acceptance of the detector in ϕ, so a first-order lifetime bias due to alignment errors is possible. However, this bias is negligible in our case because only a small fraction of the entire event sample was collected in the period of incomplete acceptance, and I subtract the measured d_0 offsets (section 6) before making the lifetime measurement.

6 Systematic d_0 offsets

As in previous years, systematic offsets are removed from the measured d_0's of the τ daughter tracks. The offsets are mapped in bins of θ and ϕ by simply measuring the average d_0 with respect to the beam axis of selected tracks in $q\bar{q}$ events. The TPC, ITC, and VDET hit requirements imposed in this selection are identical to those employed in the lifetime analysis.

In 1993, the offsets vary smoothly with ϕ (fig. 2). The map is constructed from 1.79 million tracks with 20 bins in θ and 50 bins in ϕ. The offset in a particular bin is measured with a statistical uncertainty of about $5\,\mu$m. The rms of the offsets removed from the reconstructed tracks in the selected real 1-1 events is $12\,\mu$m.

The offsets are larger in 1994 (fig. 3), and there are pronounced structures in the region of face 9 in the inner layer of VDET (about $310° < \phi < 354°$). The explanation of these features was provided by Gary Taylor: face 9 was removed from the detector between the 1993 and 1994 run periods but it was inadvertently replaced backwards, i.e., with the two modules interchanged. As a result, the bonding maps used to determine VDET strip positions in `julia` were mixed up and the VDET hit coordinates were incorrectly measured.

The TPC gating problems have a noticeable effect on the d_0 offsets in the relevant (now excluded) regions of the detector. Elsewhere the shapes of the offset maps are essentially identical before and after run 26330, but there are global shifts between the two periods ($-3\,\mu$m in End A and $+5\,\mu$m in End B for "after" minus "before"). I therefore use runs ≥ 26330 to build the offset maps for the τ lifetime analysis, and I correct for the global shifts in the earlier runs. The map has narrow ϕ bins (0.6°) in the two regions of violent behavior and the usual 7.2° bins elsewhere; 20 θ bins are used everywhere. A total of 4.14 million tracks are selected in the runs after the TPC gating problem; the statistical uncertainties are $10\,\mu$m and $3\,\mu$m in the fine and coarse bins, respectively. The rms of the offsets, measured from the accepted 1-1 events in runs ≥ 26330, is $14\,\mu$m.

Samples of $e^+e^- \to \mu^+\mu^-$ events in the data are used to check the d_0 resolution. In 1993, the impact parameter sum distribution has a fitted σ of $33.25 \pm 0.24\,\mu$m before the offsets are subtracted and $30.92 \pm 0.23\,\mu$m after. In 1994 the σ's are $34.62 \pm 0.17\,\mu$m before and $32.29 \pm 0.16\,\mu$m after.

7 Parametrization of the d_0 resolution

An estimate of the d_0 resolution for each of the daughter tracks is used in the computation of the event weights for the lifetime fit. Unlike the IPS-like methods, the IPD method is quite insensitive to the assumed d_0 resolution. To first order the fitted slope of $\langle Y \rangle$ vs. X is the same for any subsample of events; the weights may be defined arbitrarily, but one would obviously like to choose them so as to minimize the uncertainty on the fitted slope. I must therefore estimate the total smearing on the impact parameter difference, of which the tracking resolution is one component. I use the parametrization scheme devised by A. Lusiani *et al.* [6,8] and used for the IPS [9] and MIPS [10] analyses. In

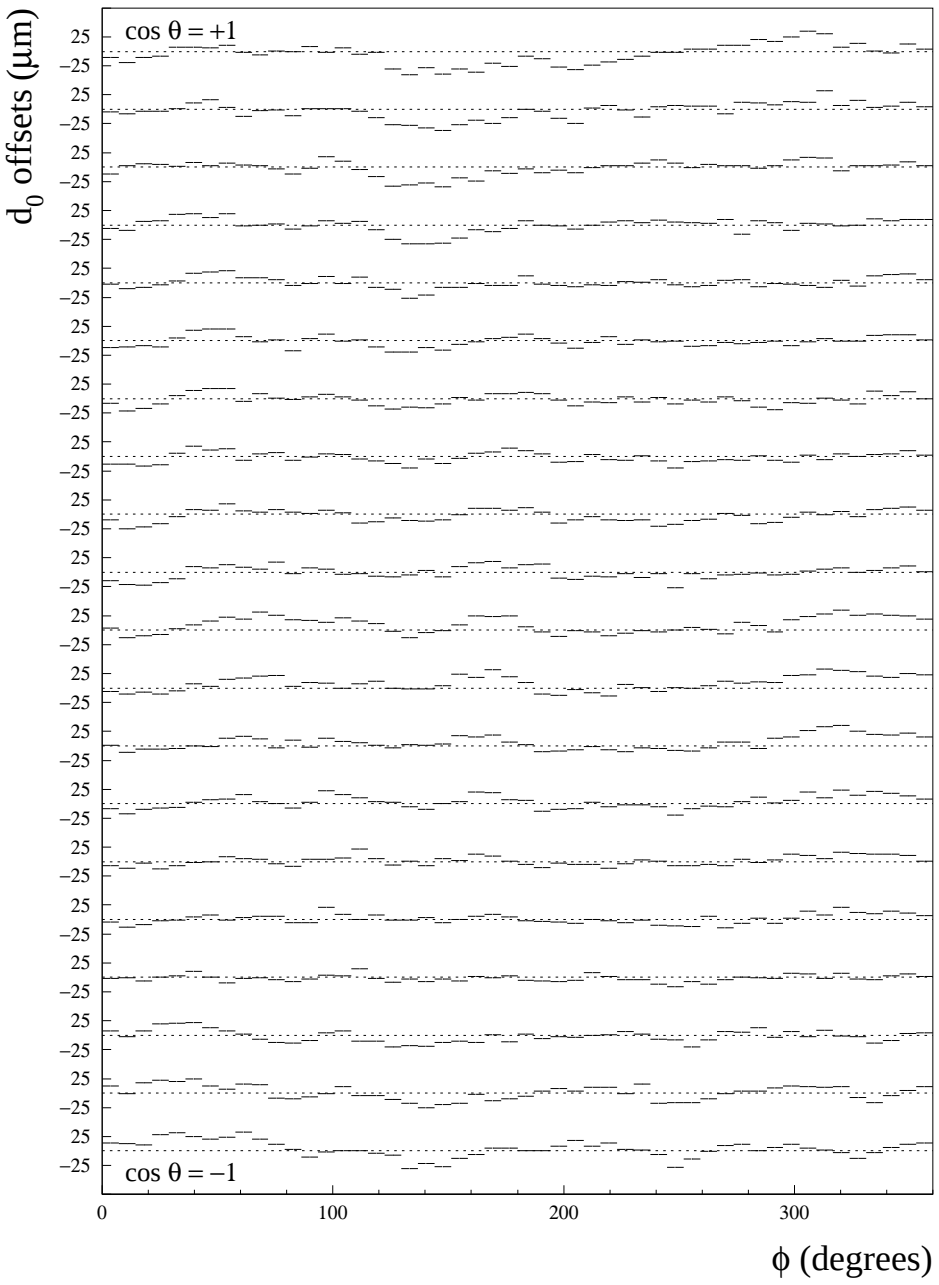

Figure 2. $\langle d_0 \rangle$ vs. ϕ for selected tracks from $q\bar{q}$ events collected in 1993. The twenty histograms represent (unequal) slices in $\cos\theta$, from $+1$ (top) to -1 (bottom).

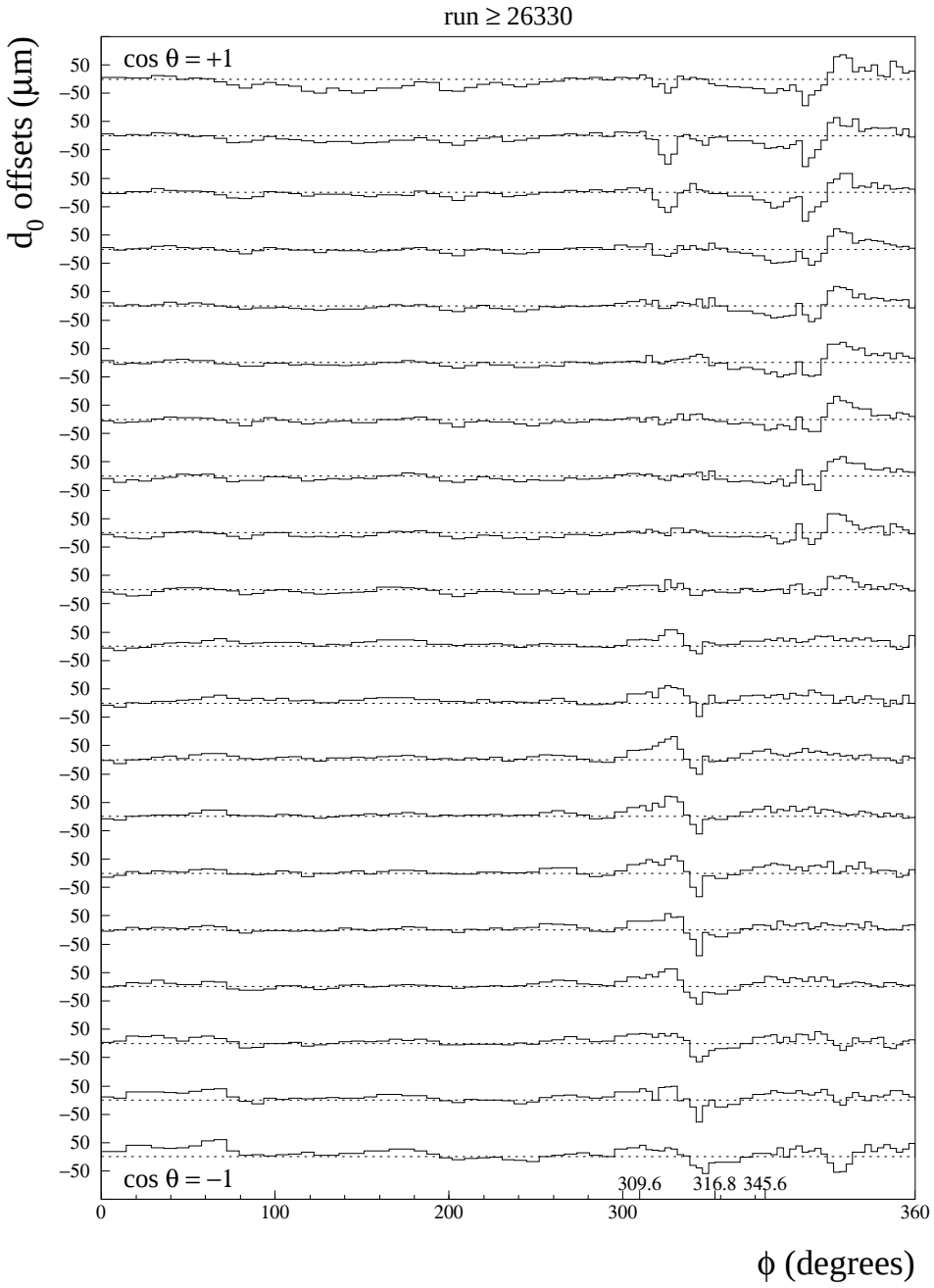

Figure 3. $\langle d_0 \rangle$ vs. ϕ for selected tracks from $q\bar{q}$ events collected in 1994 (run $\geq$ 26330). In this figure the horizontal scale of the histograms is expanded in the regions $309.6° \leq \phi < 316.8°$ and $345.6° \leq \phi < 360°$, where the map is constructed with finer binning. Note also that the vertical scale is compressed with respect to fig. 2.

this scheme, the d_0 resolution function is taken to be the sum of three Gaussian functions whose parameters depend on the d_0 uncertainty calculated by `julia` and on the track momentum, polar angle, and configuration of VDET r-ϕ hits (inner layer only, outer layer only, or both layers). The constants used to represent the real data are determined (by Alberto) from samples of $e^+e^- \to e^+e^-$, $\mu^+\mu^-$ and $\gamma\gamma \to e^+e^-$, $\mu^+\mu^-$ events. The resolution constants used in the Monte Carlo analysis to measure the biases of the method would ideally be determined in the same way from Monte Carlo e^+e^- and $\mu^+\mu^-$ samples. However, at the present time no $\gamma\gamma$ Monte Carlo events are available that reproduce the tracking conditions found in the large $\tau^+\tau^-$ Monte Carlo samples for 1993 and 1994[1]. Instead I use constants extracted from the $\tau^+\tau^-$ Monte Carlo events themselves. The d_0 errors (i.e., the smearing of the d_0's, not the uncertainties calculated by `julia`) are roughly 15% larger in the 1994 Monte Carlo than in the 1993 Monte Carlo.

Because the far tails of the tracking resolution are reduced by the trimming procedure in the lifetime fit, the third Gaussian function is omitted from the calculation of the d_0 resolution for each track; the rms of the sum of the first two Gaussian functions is taken as the resolution (σ).

8 Extra d_0 smearing for Monte Carlo events

As in the past, the impact parameter resolution found in the Monte Carlo events is generally better than that observed in the real data. Since the correlated tracking errors on d_0 and ϕ_0 introduce a bias on the fitted mean decay length, I endeavor to make the simulation more accurate by adding extra smearing to the track fit results in Monte Carlo events before performing the lifetime fits. The amount of extra d_0 smearing to be applied to a reconstructed Monte Carlo track is determined as follows. First, the d_0 uncertainty of the track is calculated from the parametrization described in section 7. Next, the uncertainty is recalculated from the same `julia` uncertainty, track momentum, θ, and hit configuration, but using the parameters corresponding to the *real data* of the same run period. If the resolution for the track in question is expected to be worse in data than in Monte Carlo, the quadratic difference of the resolutions is used to generate an extra smearing in the Monte Carlo analysis and the larger σ value is used in the calculation of the event weight. An error in ϕ_0, correlated to the extra d_0 smearing, is also added: $\delta\phi_0 = \delta d_0/10\,\mathrm{cm}$. If the resolution is already expected to be worse in Monte Carlo, no additional smearing is applied. The effect of the extra smearing on the lifetime is on the order of 0.1%.

This implementation of extra smearing affects the width of the core of the simulated d_0 resolution, but cannot compensate for discrepancies in the tails. As will be shown in section 12.8, the $\tau^+\tau^-$ Monte Carlo underestimates the number of mismeasured hadrons in the far tails.

[1] We do have $\gamma\gamma$ Monte Carlo events to match a small obsolete $\tau^+\tau^-$ production from 1993; those events were used in the MIPS analysis that was approved for Warsaw [11].

9 Event Selection

The event selection algorithm has undergone only minor changes since the analysis of the 1992 data [3]:

- The non-standard detector status variable `slumok .OR. llumok` has been abandoned in favor of the conventional `xlumok`.
- The $\tau^+\tau^-$ selection routine `tslt02` is now used instead of `tslt01`.
- `qdedx` is now used instead of `qdedxm` for analyzing Monte Carlo events. (This is relevant for electron identification in the bremsstrahlung rejection algorithm.)
- A cut on the invariant mass of each hemisphere is used to reject events containing final state radiation (emitted from the τ's). In the past the invariant mass was calculated from the one "good" charged track and any photons in the hemisphere. In order to improve the rejection of final state radiation if the photon converts in the detector material, any additional charged energy-flow tracks (including tracks from V^0's) that may be present are now included in the calculation. This change reduces the rms acoplanarity of the accepted τ pairs from 6.20 mrad to 6.07 mrad (at the peak) while reducing the efficiency by less than 0.1%.

The numbers of events surviving each step of the selection algorithm are given in table 3. For technical reasons, the cuts are applied in a different order than in [3]. The table shows that the efficiency of the cut on the helix fit χ^2 per degree of freedom is poorly modeled, as in past years. I now understand that this problem is caused by crazy TPC coordinates (probably due to delta rays) which are not accurately simulated. This is discussed further in section 12.8.

Significant discrepancies are also seen for the Bhabha rejection and bremsstrahlung rejection cuts. The problem with the `bhasel` cut is not significant because most Bhabha events that survive this cut are later killed; usually one or both of the tracks pass outside the $\cos\theta$ range of VDET or undergo bremsstrahlung. The discrepancy in the bremsstrahlung rejection cut is discussed in section 12.8.

The Monte Carlo predictions for the efficiencies of the ITC and VDET hit requirements are higher than those observed in the real data. In the 1-1 selection, about 0.7% of the tracks fail the ITC hit requirement, usually because extra tracks from a nuclear interaction or photon conversion are present or the track is kinked at the ITC/TPC interface. The discrepancy between data and Monte Carlo is at the level of 0.1% per track. A study of the efficiency of the ITC hit requirement in Bhabha and dimuon events shows a smaller discrepancy in the opposite direction; in these events only about 0.1 to 0.2% of the tracks fail the ITC hit requirement. This study confirms that the discrepancy in the $\tau^+\tau^-$ Monte Carlo is related to extra tracks or scattering, both of which are covered in section 12.8.

On the other hand, the efficiency of the VDET hit requirement is consistently too high in the Bhabha, dimuon, and $\tau^+\tau^-$ Monte Carlo samples. I can think of two possible sources for such a universal discrepancy: (1) inefficient or dead channels in VDET or (2) a mismeasurement in the ITC or TPC that causes the VDET hits to be missed. The first

Table 3. Numbers of events surviving each selection criterion in data and Monte Carlo, for the combined 1993 and 1994 samples. The Monte Carlo includes τ pairs and backgrounds. The Monte Carlo numbers are normalized to correspond to the size of the real data samples, as specified in table 1. $\epsilon_{\rm data}$ is the fraction of events passing a cut in the real data. The last column contains $\epsilon_{\rm data}/\epsilon_{\rm MC}$, the ratio of the fractions of events passing each cut in data and Monte Carlo.

Cut	Data	MC	$\epsilon_{\rm data}$	$\epsilon_{\rm data}/\epsilon_{\rm MC}$
Class 24	646556			
`xlumok`	638313			
`xvdeok`	637758			
No online error	637749			
`tslt02`	90408	90666		
Rejected by `bhasel`	88986	89533	0.9843 ± 0.0004	0.9967 ± 0.0004
1-1 topology	51985	52551	0.5842 ± 0.0017	0.9953 ± 0.0030
Opposite charges	51369	51967	0.9882 ± 0.0005	0.9993 ± 0.0005
Tracks accepted by `enflw`	51342	51931	0.9995 ± 0.0001	1.0002 ± 0.0001
≥ 8 TPC hits	51087	51697	0.9950 ± 0.0003	0.9995 ± 0.0003
≥ 4 ITC hits	50373	51080	0.9860 ± 0.0005	0.9979 ± 0.0006
≥ 1 VDET r-ϕ hit	48562	49488	0.9640 ± 0.0008	0.9951 ± 0.0009
$\chi^2/{\rm dof} < 5$	47103	49295	0.9700 ± 0.0008	0.9738 ± 0.0008
$p > 1\,{\rm GeV}/c$	45483	47567	0.9656 ± 0.0008	1.0007 ± 0.0009
Bremsstrahlung rejection	43011	45292	0.9457 ± 0.0011	0.9931 ± 0.0012
≤ 2 extra tracks per hemi	41954	44216	0.9754 ± 0.0007	0.9992 ± 0.0008
Isolated photon rejection	40077	42192	0.9553 ± 0.0010	1.0011 ± 0.0011
Exclusion zones	38457	40518	0.9596 ± 0.0010	0.9992 ± 0.0011
$\lvert X\rvert < 0.18$ (fit range)	38120	40211	0.9912 ± 0.0005	0.9988 ± 0.0005

kind of problem would be of no consequence for the lifetime measurement. The second kind of problem could affect the lifetime if it degraded the impact parameter resolution for the tracks with VDET hits; such issues are discussed in section 12.8.

Events with $|X| \geq 0.18$ are excluded from the fit in order to reduce the effects of the $\sin\psi = \psi$ approximation (section 12.3) and of background events from two-photon interactions. A total of 38120 events enter the fit, 11192 from 1993 and 26928 from 1994.

10 Fit to the Y vs. X Distribution

Figure 4 shows the Y vs. X distribution for the accepted events in the 1993 and 1994 data. The usual iterative trimming procedure is used to fit the function $Y = a_0 + a_1 X$ to the data; each year is fitted separately. The trim value $\Delta_{\rm trim}$ is set to 0.137 cm as in the 1992 analysis. In any iteration of the fit, the events with residuals $\Delta_i = Y_i - a_0 - a_1 X_i$

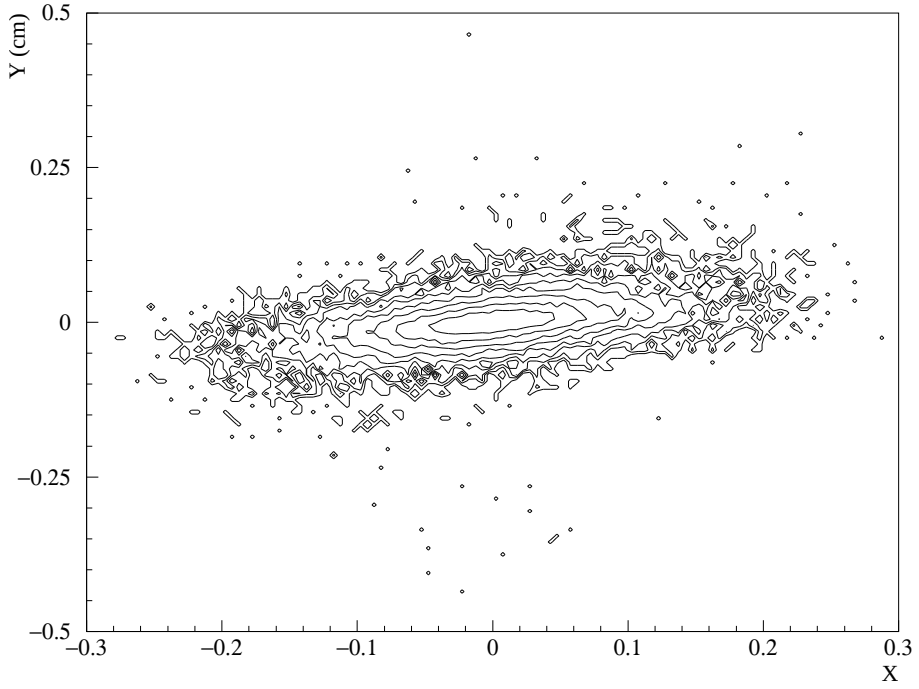

Figure 4. Contour plot of the Y vs. X distribution from the 1993 and 1994 data.

satisfying $|\Delta_i| < \Delta_{\rm trim}$ are considered, where a_0 and a_1 are the results from the previous iteration. After the fits converge, the trimming in the final iteration removes 0.21% of the events in the 1993 data within the fitted range of X, and 0.20% in 1994. In the Monte Carlo samples 0.16% of the events are removed; if the tails are enhanced as discussed in section 12.8 the fraction increases to 0.19% in 1993 and 0.20% in 1994.

The event weights $w_i = 1/\sigma^2(Y_i)$ are computed as before. The contributions to $\sigma(Y_i)$ are d_0 resolution including all sources of tracking errors (typically 75 μm for two tracks); beam size and position (typically 230 μm in 1993 and 180 μm in 1994); and the natural spread caused by the exponential τ decay time distribution (typically 120 μm, smaller near $X = 0$, larger at large $|X|$). The total smearing on Y is typically 270 μm in 1993 and 230 μm in 1994.

The fitted data are shown in figs. 5 and 6. The fit results for 1993 are

$$\begin{aligned} a_1 &= 0.21987 \pm 0.00448\,\text{cm}, \\ a_0 &= 0.00070 \pm 0.00019\,\text{cm}, \end{aligned}$$

with $\chi^2 = 11658$ for 11167 degrees of freedom; for 1994 I obtain

$$\begin{aligned} a_1 &= 0.22245 \pm 0.00271\,\text{cm}, \\ a_0 &= 0.00035 \pm 0.00011\,\text{cm}, \end{aligned}$$

with $\chi^2 = 27162$ for 26871 degrees of freedom.

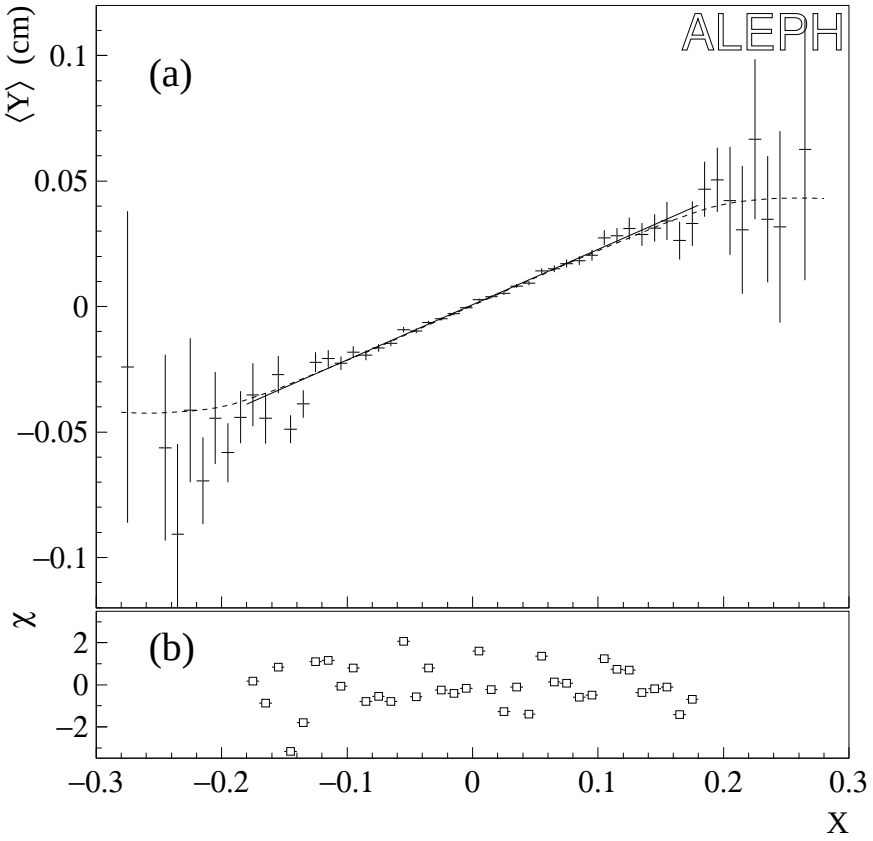

Figure 5. (a) $\langle Y \rangle$ vs. X for the 1993 data. The solid line shows the result of the fit described in the text. For $|X| < 0.18$, the plotted $\langle Y \rangle$ values are computed after trimming in the final iteration of the fit. For display purposes, the data at $|X| > 0.18$ have been trimmed at the same Δ_i values. The dashed curve shows the expected shape of $\langle Y \rangle$ vs. X. To obtain this curve from Monte Carlo, I rescaled the τ lifetime to match the value measured in the data, added background (setting $Y = 0$ to reduce fluctuations), antisymmetrized, and smoothed the function. (The small positive offset in Y due to bremsstrahlung was preserved in the antisymmetrization process.) (b) Pull for each bin of (a) (deviation from fitted line divided by uncertainty).

11 Statistical uncertainty on the lifetime

The statistical uncertainty on the lifetime is given by $\Delta\tau_\tau = \Delta a_1 \times (d\tau_\tau / da_1)$, where Δa_1 is the uncertainty on the fitted slope a_1. The values of Δa_1 given in section 10 were calculated by the fitting program. A simple Monte Carlo program is used to perform an independent calculation of these uncertainties. The distributions of the pulls (residual in Y divided by uncertainty on Y) for events with $X < 0$ and $X \geq 0$ are separately extracted from the real data of each year. These distributions are used to generate 4000 random samples of $\{Y_i\}$, where the $\{X_i\}$ and weights from the real data are reused in each sample. The resulting collections of a_1 values have rms $= 0.00465 \pm 0.00005$ cm in 1993 and 0.00271 ± 0.00003 cm in 1994. I take 0.00465 and 0.00271 as the statistical errors on

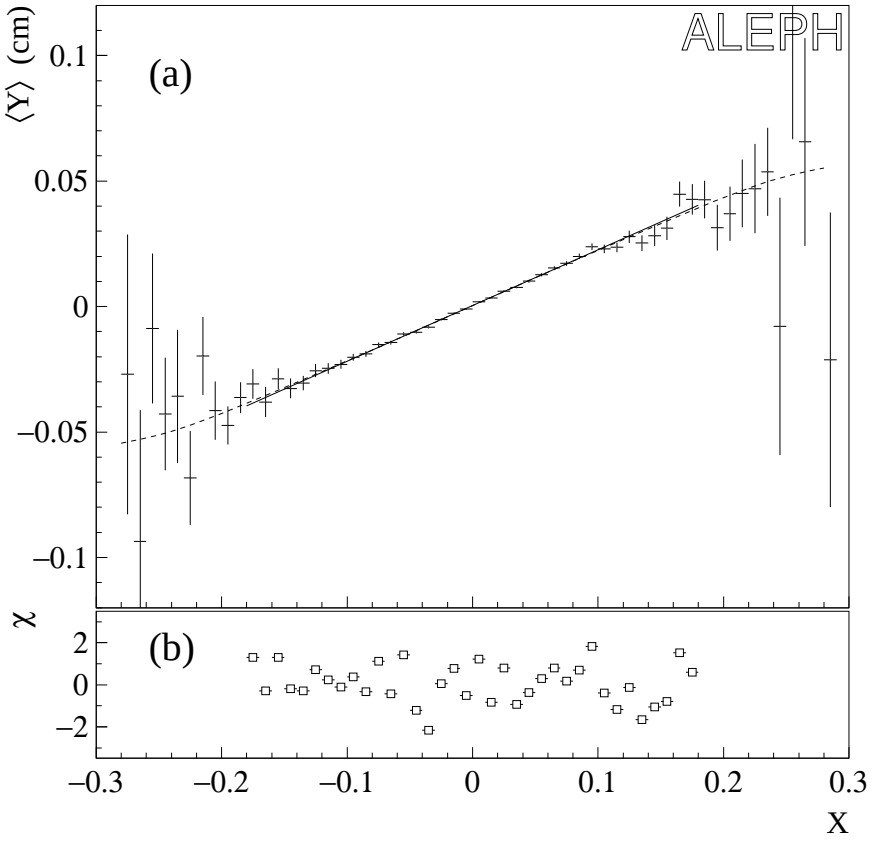

Figure 6. (a) $\langle Y \rangle$ vs. X for the 1994 data. (b) Pull for each bin of (a).

the respective values of a_1 obtained from the data.

The derivative $da_1/d\tau_\tau$ is obtained by differentiating equation 5:

$$\frac{da_1}{d\tau_\tau} = \frac{\vec{p}^{\,0}_\tau}{M_\tau}\left(1 + D + \tau_\tau \frac{dD}{d\tau_\tau}\right). \tag{6}$$

The bias D and its derivative are computed from Monte Carlo events, including background channels. The $\tau^+\tau^-$ Monte Carlo is generated with a single τ_τ value of 296 fs. In order to simulate other lifetimes, I rescale the true impact parameters of the daughter tracks, measured with respect to the Z^0 production point, while keeping fixed the individual impact parameter measurement errors (reconstructed minus true). The τ lifetimes in each event are generated five times to increase the Monte Carlo statistics, while the angles and measurement errors are reused. This leads to a 10% reduction in the statistical uncertainty on the bias. The bias calculation is iterated so that the bias and derivative used to analyze each year correspond to the corrected lifetime measured in the real data. For 1993 I find $D = -0.58 \pm 0.26_{\rm stat}\%$ and $\tau_\tau\, dD/d\tau_\tau = -0.029$; for 1994 the results are $D = -0.19 \pm 0.25_{\rm stat}\%$ and $\tau_\tau\, dD/d\tau_\tau = -0.032$.

The statistical uncertainty on the lifetime is then $\Delta\tau_\tau = 6.29$ fs in 1993 and 3.66 fs in 1994.

12 Systematic Errors

The fitted mean decay length is affected by certain biases for which corrections must be made. The biases are computed individually from Monte Carlo events, as in past years. The biases from the 1993 and 1994 Monte Carlo samples are evaluated separately, and the corresponding corrections are applied separately to the slopes measured from the respective data samples. The procedure is described in detail in [3]. Systematic differences between data and Monte Carlo are also taken into account. The biases and other sources of systematic error are discussed in this section and are itemized in table 4.

12.1 Selection bias

This bias is measured by comparing the sample means of the Monte Carlo τ lifetimes before and after the event selection is performed.

Idealized X and Y variables, derived from Monte Carlo truth information, were defined in [3]. It was argued that the fitted mean decay length $L_{\rm D}$ obtained from these variables is related to the sample mean lifetime $\tau_{\rm C}$ by $L_{\rm D} = \tau_{\rm C}\bar{p}^0_\tau/M_\tau$. In other words, the selection bias is independent of X. This fact allows one to reduce the statistical uncertainty on the lifetime bias obtained from the Monte Carlo.

As a cross check, I calculate the "X-dependent selection bias" from the Monte Carlo: $+0.10 \pm 0.35\%$ in 1993 and $-0.16 \pm 0.29\%$ in 1994. These values are consistent with zero, as expected.

12.2 p_τ vs ψ correlation

Events with initial or final state radiation tend to have shorter τ decay lengths. They also tend to have larger decay angles ψ and hence yield a broadened X distribution. The resulting X dependence of the mean τ momentum gives rise to a bias on the fitted mean decay length.

12.3 $\sin\psi = \psi$ approximation

Implicit in equation 3 is the assumption that the laboratory angles $\psi = \phi_{\rm daughter} - \phi_\tau$ are small. These angles are typically $1/\gamma_\tau$ radians, where γ_τ refers to the boost of the τ in the lab frame. Without radiation, $\gamma_\tau = 25.7$ at the $\rm Z^0$ peak. The resulting bias is on the order of 0.1%. As the X distribution (and hence the ψ distribution) is adequately simulated (fig. 7), no additional systematic uncertainty is assigned.

12.4 Acoplanarity of τ^+ and τ^-

Equation 3 is based on the assumption that the τ^+ and τ^- are back to back in xy projection. A relatively small number of events with final state radiation survive the

Table 4. Systematic biases and errors in the τ lifetime measurement. Sources assumed to give fully correlated contributions in 1993 and 1994 are marked "corr". Contributions listed as "negligible" are smaller than 0.05%.

	$\Delta\tau_\tau/\tau_\tau$ (%)	
Description	1993	1994
Selection bias	$+0.11 \pm 0.15$	-0.06 ± 0.14
p_τ vs. ψ correlation	-0.15 ± 0.03	-0.14 ± 0.02
$\sin\psi = \psi$ approximation	-0.12 ± 0.01	-0.12 ± 0.01
Acoplanarity of τ^+ and τ^- (MC)	-0.35 ± 0.04	-0.32 ± 0.03
Acoplanarity of τ^+ and τ^- (syst)	$\pm 0.09_{\rm corr}$	$\pm 0.09_{\rm corr}$
θ measurement errors	negligible	negligible
ϕ_0 resolution	-0.08 ± 0.02	-0.08 ± 0.01
Beam position and size	negligible	negligible
d_0 resolution & trimming (MC)	$+0.31 \pm 0.21$	$+0.73 \pm 0.20$
Hadron d_0 resolution tails (syst)	$\pm 0.17_{\rm corr}$	$\pm 0.28_{\rm corr}$
d_0 resolution core and near tails	$\pm 0.09_{\rm corr}$	$\pm 0.09_{\rm corr}$
Detector alignment	$\pm 0.11_{\rm corr}$	$\pm 0.16_{\rm corr}$
Bremsstrahlung	$\pm 0.11_{\rm corr}$	$\pm 0.11_{\rm corr}$
Nuclear interactions	negligible	negligible
Confusion due to extra tracks	$\pm 0.20_{\rm corr}$	$\pm 0.20_{\rm corr}$
Trimming	negligible	negligible
$q\bar{q}$ background	negligible	negligible
$e^+e^- \to e^+e^-$ background	$+0.01 \pm 0.02$	0.00 ± 0.01
$e^+e^- \to \mu^+\mu^-$ background	-0.01 ± 0.01	-0.01 ± 0.01
$\gamma\gamma \to \ell^+\ell^-$ background	-0.29 ± 0.08	-0.19 ± 0.04
Cosmic ray background	negligible	negligible
Background (syst)	$\pm 0.07_{\rm corr}$	$\pm 0.05_{\rm corr}$
τ branching fractions	negligible	negligible
Other τ topologies	negligible	negligible
τ mass	negligible	negligible
Average τ momentum	negligible	negligible
Determination of θ	negligible	negligible
Detector dimensions	negligible	negligible
VDET strip pitch	negligible	negligible
Track curvature	negligible	negligible
Beam axis offset	negligible	negligible
Variation of fit X range	negligible	negligible
Total bias	$-0.58 \pm 0.27 \pm 0.34_{\rm corr}$	$-0.19 \pm 0.25 \pm 0.42_{\rm corr}$

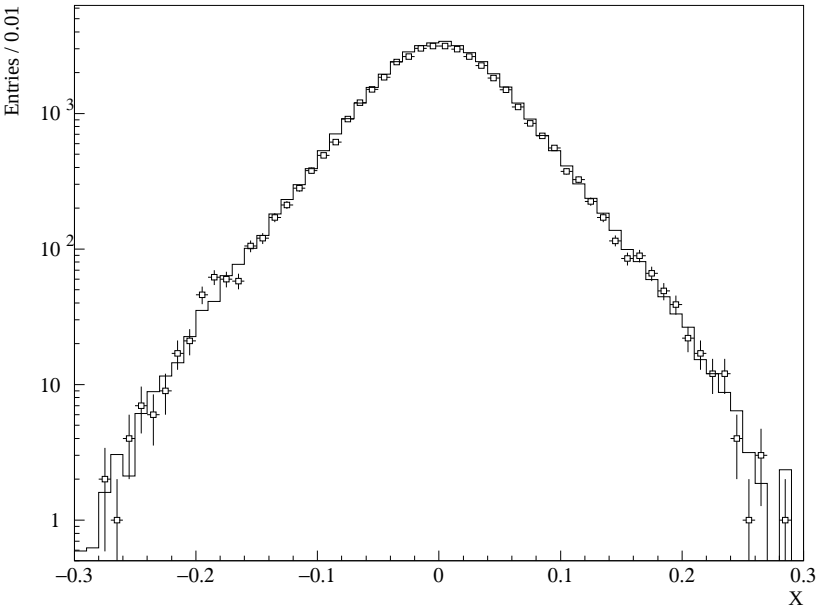

Figure 7. Distribution of X, after all cuts, for 1993 and 1994 data (squares with error bars) and Monte Carlo (histogram). The rms is 0.0573 in data and 0.0568 in Monte Carlo, a marginally significant difference of 0.9%. Throughout this memo, all Monte Carlo plots are normalized to the integrated luminosities in table 1 and include backgrounds, unless otherwise stated.

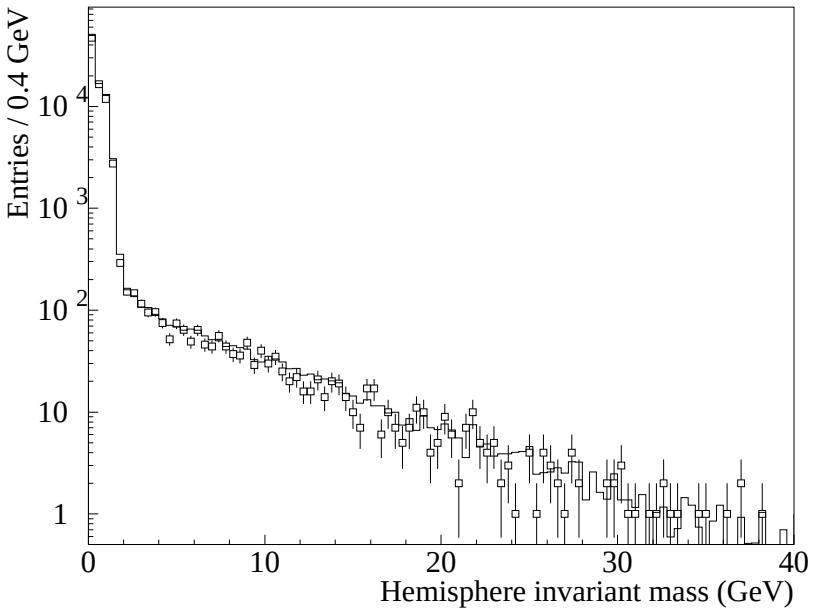

Figure 8. Hemisphere invariant mass distribution when the final state radiation cut is released, in data (squares with error bars) and Monte Carlo (histogram). (No restriction on X is imposed here.) The cut removes events containing a hemisphere with mass greater than $2\,\mathrm{GeV}/c^2$.

event selection and violate this assumption. The measured $\Delta\phi$ values for these events receive the unwanted contribution from the acoplanarity angle of the τ^+ and τ^-, which leads to a smearing in X. In other words, the X values tend to move further from zero, and the fitted slope is reduced by roughly 0.3%.

I use the distribution of hemisphere invariant mass (fig. 8) to check for systematic errors in the simulation of final state radiation. Events with hemisphere masses below $2\,\mathrm{GeV}/c^2$ are used in the lifetime measurement. The fraction of hemispheres with mass greater than $2\,\mathrm{GeV}/c^2$ is $2.27 \pm 0.05\%$ in data and $2.30 \pm 0.02\%$ in Monte Carlo. I conclude that the simulation of final state radiation is correct to within $0.05/2.27 = 2.2\%$. The fitted slope changes by -3.9% when the isolated photon cut is removed. So I take $(2.2\%) \times (3.9\%) = 0.09\%$ as a common systematic error contribution for 1993 and 1994.

12.5 θ measurement errors

Errors on θ_{thrust} due to missing neutrinos and detector resolution are negligible.

12.6 ϕ_0 resolution

Errors on the measured daughter track ϕ_0 angles yield a small broadening of the X distribution and a small reduction in the fitted slope. The relative lifetime bias is roughly given by the mean square error on X divided by $\langle X^2 \rangle$. The ϕ_0 errors are somewhat underestimated in the Monte Carlo, but this discrepancy is reduced by the extra smearing discussed in section 8, and yields a negligible systematic error.

12.7 Beam position and size

As discussed in [3], the smearing in Y related to the uncertainty on the beam axis position and the size of the luminous region cannot produce a bias on the fitted slope unless there is a hole in the acceptance in ϕ and a systematic mismeasurement of the beam axis. We do indeed have a hole in the acceptance in the early part of 1994, but the errors on the beam axis position are so small and the interval in question is so short (providing only 3% of the accepted events) that the resulting bias is negligible. The biases measured in the Monte Carlo samples, $-0.10 \pm 0.33\%$ in 1993 and $+0.02 \pm 0.31\%$ in 1994, are therefore ignored in the lifetime determination.

12.8 d_0 resolution, bremsstrahlung, etc.

Measurement errors on the track impact parameters introduce a bias on the slope. The bias results primarily from the correlation of the tracking errors on d_0 and ϕ_0 for each daughter; in the absence of trimming, the relative change in the fitted slope is roughly given by

$$\frac{\Delta\tau_\tau}{\tau_\tau} \simeq \frac{\langle \delta d_0 \, \delta \phi_0 \rangle}{\langle d_0 \psi \rangle}, \tag{7}$$

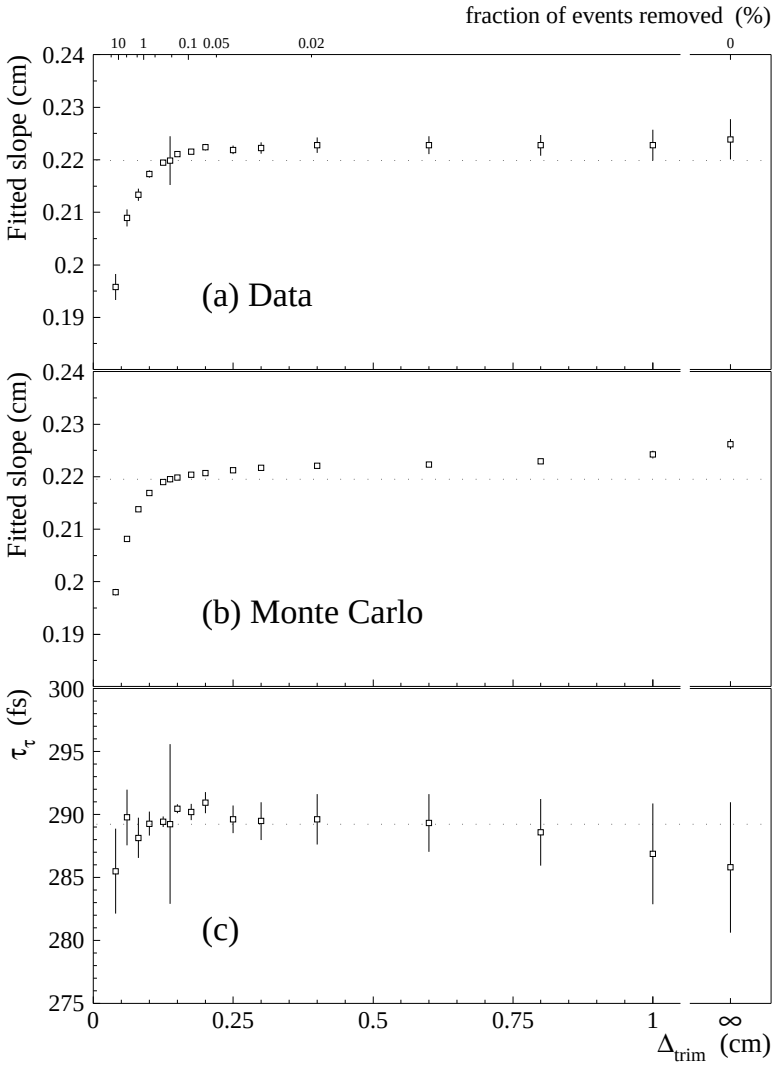

Figure 9. Fitted slope a_1 versus the trim point $\Delta_{\rm trim}$ for 1993: (a) data; (b) Monte Carlo including backgrounds. The resulting measurement of the τ lifetime is plotted versus $\Delta_{\rm trim}$ in (c). In each plot, the error bar at the nominal $\Delta_{\rm trim} = 0.137\,{\rm cm}$ represents the statistical uncertainty on the slope or lifetime. The error bars on the other points indicate the uncertainty on the variation with respect to the nominal $\Delta_{\rm trim}$.

where the numerator on the right-hand side describes the detector-induced correlation between d_0 and ϕ_0, and the denominator characterizes the lifetime-induced correlation ($\langle d_0\psi\rangle \sim 2\,\mu{\rm m}$ for $45\,{\rm GeV}$ τ's). Most daughter tracks in the sample are well measured and the corresponding bias is very small; many poorly measured tracks are removed by the trimming procedure in the lifetime fit. The remaining bias is calculated from the simulated events.

The dependence of the fitted slope on the trim point $\Delta_{\rm trim}$ is shown in figs. 9 and 10. A significant discrepancy between data and Monte Carlo is observed in 1994 for $\Delta_{\rm trim} \sim 0.2\,{\rm cm}$; a similar effect appears to be present in the lower statistics of 1993.

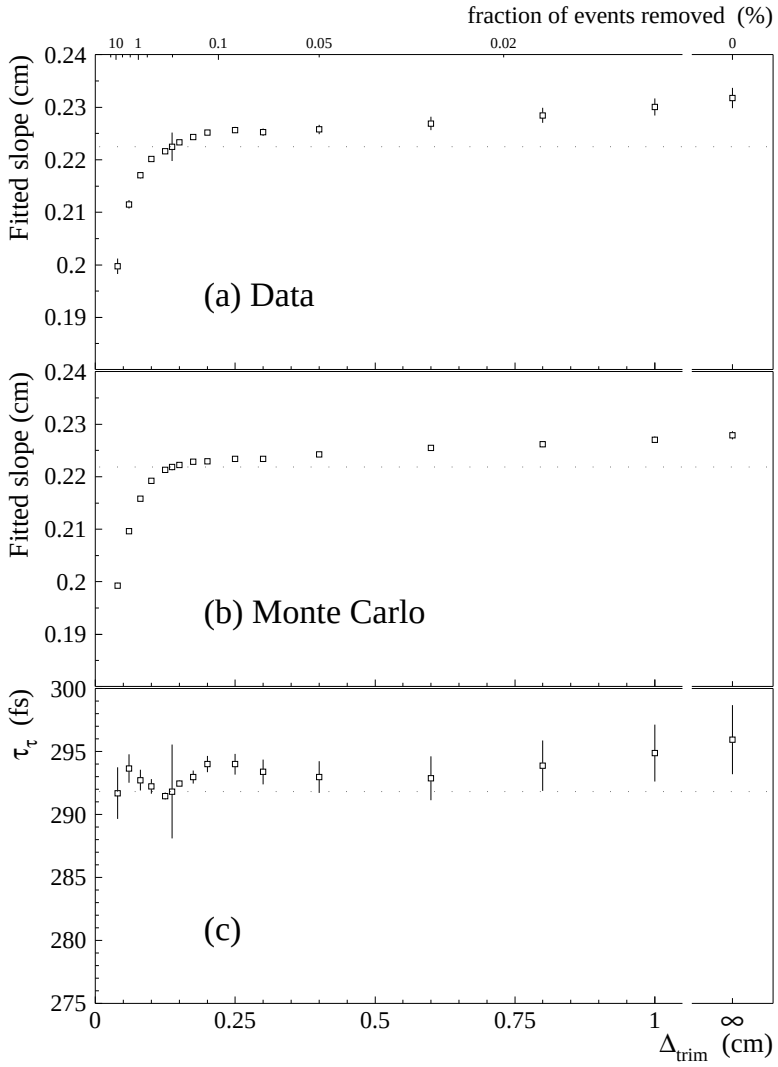

Figure 10. Fitted slope a_1 versus the trim point $\Delta_{\rm trim}$ for 1994: (a) data; (b) Monte Carlo including backgrounds. The resulting measurement of the τ lifetime is plotted versus $\Delta_{\rm trim}$ in (c).

I have investigated the discrepancy in detail. The residuals Δ of the accepted events from 1994 are plotted separately for $X < 0$ and $X \geq 0$ in fig. 11. In the data there is a small excess of events with $X \geq 0$ and $\Delta = 0.1$ to 0.2 cm.

I selected events with $0.137 < |\Delta| < 0.2$ cm for further studies; 27 such events are found in the 1994 data. The 1994 Monte Carlo predicts 19.1 events in this region, including 5.1 events with long-lived τ's, 1.5 events with nuclear interactions in the detector material (and nucleons ejected), 11.1 other events with mismeasured hadron tracks, 1.5 events with mismeasured electron tracks (including bremsstrahlung), zero events with large impact parameters due to the beam size, and zero events from background channels.

The following 2×2 histograms show the breakdown of these events for positive and

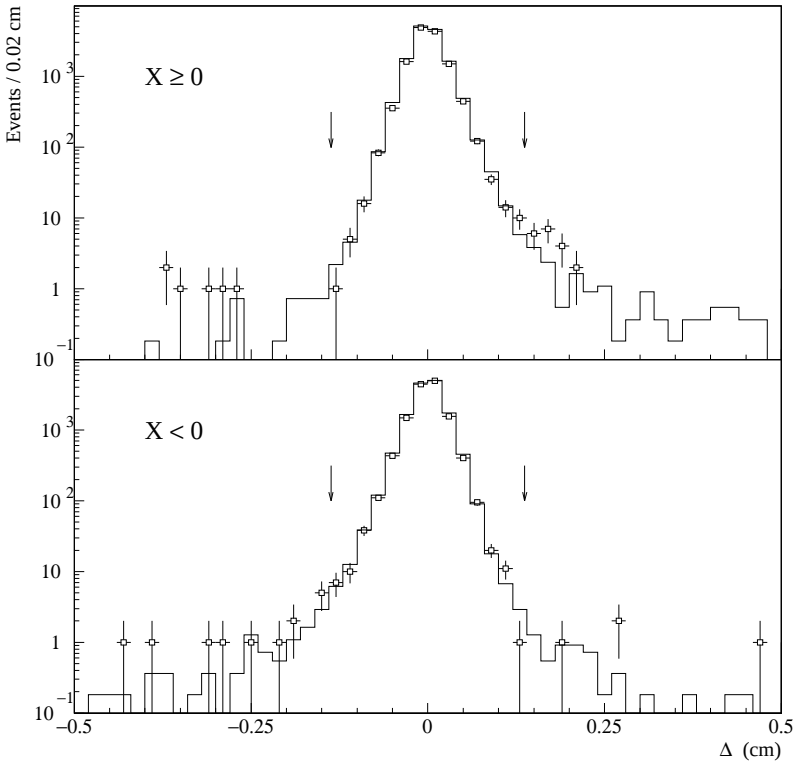

Figure 11. Residuals $\Delta_i = Y_i - a_0 - a_1 X_i$ from the 1994 data (squares with error bars) and Monte Carlo (histogram), for $X \geq 0$ (top) and $X < 0$ (bottom). Arrows mark the trim points at $\Delta = \pm 0.137$ cm.

negative Δ (on the vertical axis) and for positive and negative X (on the horizontal axis):

$$\text{Data:} \quad \begin{bmatrix} 1 & 19 \\ 7 & 0 \end{bmatrix},$$

$$\text{Monte Carlo:} \quad \begin{bmatrix} 3.1 & 7.3 \\ 6.4 & 2.4 \end{bmatrix};$$

there is a large excess in the data in the upper-right quadrant, i.e., the region $X \geq 0$, $\Delta > 0$.

I scanned the 27 events from the data. They all contain one daughter track with a huge d_0 (with respect to the beam axis) and one with a reasonable d_0, so in each case it is fairly clear which hemisphere contains the mismeasured track (or the long-lived τ). The identity of the mismeasured track could also be reliably determined: I find 6 e's, 1 μ, and 20 h's (possibly some kaons, the rest pions; no protons). The opposite hemispheres look remarkably like a random sample of one-prong τ decays. Among the 19 events with $X \geq 0$ and $\Delta > 0$, the mismeasured track is an e in 5 cases and an h in the 14 others. The Monte Carlo predicts 1.6 e's, 1.1 μ, and 4.5 h's in that quadrant. One concludes that the data contains a mild excess of e's and a very significant excess of h's in the quadrant. There is no significant discrepancy between data and Monte Carlo for any particle type in any of the other three quadrants.

Twelve of the 14 h tracks in the upper-right quadrant have VDET r-ϕ hits in only one layer. (The Monte Carlo predicts 2.9 h tracks of this kind.) Extra (bad) charged tracks are found in only three of the 14 hemispheres.

An excess of events with $X \geq 0$ and $\Delta > 0$ but not $X < 0$ and $\Delta < 0$ implies an effect involving a loss of energy as the hadron tracks pass through the detector material. What could that be? I tried unsuccessfully to find evidence for the emission of photons or π^0's by hadron tracks in the detector material. I selected h tracks with a kink in the ITC/TPC interface, but there was no significant signal of photons balancing the particle's momentum change at the kink.

I can rule out $K^\pm \to \pi^\pm\pi^0$ decays as the source of the discrepancy; the rate for this decay is too small to produce the observed excess of events, and I verified that the decay is simulated in the Monte Carlo at the appropriate level.

I can also probably reject pion bremsstrahlung as an explanation. A Monte Carlo sample of 498K muons at 45 GeV contains only two muons with bremsstrahlung in the inner part of the ALEPH detector. If that simulation is correct [and it does seem plausible from a back-of-the envelope calculation: $(M_\mu/M_e)^2 = 4 \times 10^4$] then we would expect < 1 pion in the lifetime sample to undergo bremsstrahlung in the detector material.

I conclude that the discrepancy is related to some kind of interaction of pions with the detector material. I deal with this problem by applying a patch to my fitting program so that more mismeasured tracks are simulated in fits to the Monte Carlo events. I select 0.14% of the hadron tracks with one missing VDET hit and generate new values of X and Y with a uniform distribution on $0 < X < 0.18$ and $0.1 < \Delta < 0.2$ cm. The "natural" part of the uncertainty on Y depends on X, so the event weight is recalculated according to the new X value. The fraction of tracks selected is designed to compensate for the deficit of events of this type (2.9 vs. 12) seen in the Monte Carlo in $0.137 < \Delta < 0.2$ cm. This operation is the "enhancement of the tails" mentioned in section 10. The enhancement is used to extract the final biases from 1993 and 1994 Monte Carlo events. Figure 12 shows that the measured τ lifetime no longer depends significantly on $\Delta_{\rm trim}$ above 0.137 cm.

The errors on d_0 due to tracking resolution are now found to shift the fitted slope in $\tau^+\tau^-$ Monte Carlo events by $+3.78 \pm 0.53\%$ in 1993 and $+4.05 \pm 0.41\%$ in 1994. If trimming at $\Delta_{\rm trim} = 0.137$ cm is then added, a shift of $-3.47 \pm 0.45\%$ is observed in 1993 and $-3.32 \pm 0.34\%$ in 1994. The net biases are $+0.31 \pm 0.21\%$ and $+0.73 \pm 0.20\%$, respectively. The bias is expected to be slightly (roughly 0.1%) more positive in 1994 due to the worse d_0 resolution (because of the larger detector-induced correlations between X and Y) and the smaller beam size (because fewer long-lifetime and mismeasured events are pushed beyond the trim point by the beam-related smearing).

The systematic uncertainty associated with the tail enhancement is evaluated by extending the enhanced region to $0 < \Delta < 0.2$ cm, with proportionately more events "scattered". The net biases from d_0 resolution and trimming become $+0.47 \pm 0.20\%$ in 1993 and $+0.87 \pm 0.20\%$ in 1994. With the enhancement switched off entirely the biases are $+0.14 \pm 0.20\%$ and $+0.45 \pm 0.20\%$, respectively. From these results I assign systematic uncertainties of $\pm 0.17\%$ in 1993 and $\pm 0.28\%$ in 1994, with 100% correlation assumed between the errors in the two years.

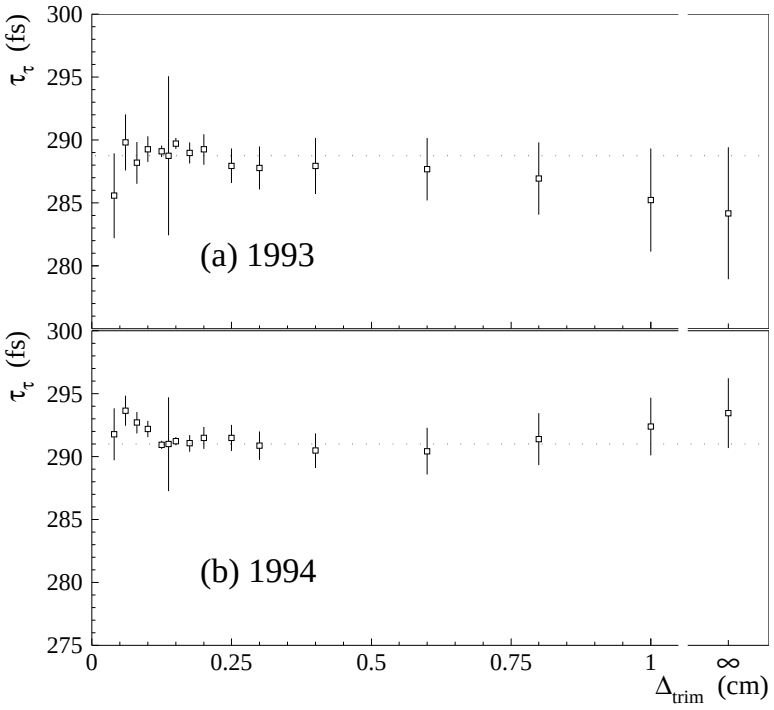

Figure 12. Measured lifetime versus $\Delta_{\rm trim}$ after the "tail enhancement" described in the text; (a) 1993; (b) 1994.

Figure 12 shows that a 2σ discrepancy between the 1994 data and Monte Carlo remains for $\Delta_{\rm trim}$ values around $600\,\mu$m. In this region the trimming induces a bias on the fitted slope of around -5%, with the data and Monte Carlo variations differing by about 0.9%. The discrepancy suggests that the d_0 resolution is still not accurately simulated in the Monte Carlo. (The beam size or the natural width of the exponential lifetime distribution also contribute to the smearing in Y, but the simulation of these elements is probably more reliable that of the d_0 resolution.) In fact, the d_0 resolution for tracks with hits in both VDET layers seems to be roughly 10% worse in the 1994 Monte Carlo than in the data; this is not corrected by my "extra smearing" scheme (section 8). Nevertheless the effect on the lifetime is very small when the trim point is set to 0.137 cm: if I reduce all d_0 errors and resolutions by 10% in the 1994 Monte Carlo, the bias on the slope changes by $-0.05 \pm 0.04\%$. If I remove the extra smearing, the value of a_1 is shifted by $0.00 \pm 0.09\%$ in the 1993 Monte Carlo and $-0.07 \pm 0.05\%$ in 1994. I take 0.09% as the systematic uncertainty on the lifetime related to the core and near tails of the d_0 resolution.

The following topics related to d_0 resolution are also discussed in this section: d_0 offsets (alignment errors), bremsstrahlung, nuclear interactions, and confusion due to extra tracks.

Alignment errors. As shown in section 6, impact parameter measurements are subject to θ- and ϕ-dependent offsets caused by errors in detector alignment or field parametrization. We have believed for some time that the d_0 offsets can produce no first-order lifetime bias if the acceptance in ϕ is 100%. I now understand that this is not exactly true for IPD because the event weights tend to have a particular ϕ dependence due to the shape

of the luminous region, possibly preventing an exact cancelation of the lifetime errors when integrating over all ϕ. Nevertheless, there is nothing to worry about in the present analysis because the offsets are first subtracted from the measured d_0's; the lifetime bias should be reduced to a negligible level. I nevertheless assign a systematic uncertainty on the lifetime corresponding to half the effect of the offset corrections.

I don't know whether the d_0 offsets in the real detector are accompanied by correlated ϕ_0 offsets, so I use the Monte Carlo to estimate the size of the effect with and without the ϕ_0 offsets. For the 1993 offset map, the lifetime shifts by $-0.17 \pm 0.05\%$ when the d_0 offsets are introduced, and $-0.05 \pm 0.05\%$ when d_0 and ϕ_0 offsets are added with $\delta\phi_0 = \delta d_0/6.3\,\mathrm{cm}$. (The inner VDET layer is at a radius of 6.3 cm.) I consider these two situations to represent the extreme cases. In the data, the fitted slope shifts by $-0.36 \pm 0.18\%$ when the offset corrections are removed, where the uncertainty reflects the expected fluctuations as calculated with the Monte Carlo. I use the larger Monte Carlo shift (without ϕ_0 offsets) to assign a systematic uncertainty of $(0.17 + 0.05\%)/2 = 0.11\%$ for detector alignment in 1993.

For the 1994 offset map, the lifetime shifts by $+0.01 \pm 0.07\%$ when the d_0 offsets are introduced, and $+0.24 \pm 0.07\%$ when d_0 and ϕ_0 offsets are added; the shift in the data is $-0.11 \pm 0.16\%$. I assign a systematic uncertainty of $(0.24 + 0.07\%)/2 = 0.16\%$ in 1994.

Bremsstrahlung. The systematic uncertainty from the simulation of bremsstrahlung is assigned from the data of fig. 13, which shows the estimated impact parameter shift for electron candidates, as calculated by the bremsstrahlung rejection program. The fraction of electron candidates failing the hard bremsstrahlung cut is 0.1266 ± 0.0024 in data and 0.1150 ± 0.0009 in Monte Carlo. The change in the fitted slope when the cut is released is $+0.82 \pm 0.17\%$ in the 1993 Monte Carlo. In the 1993 data the shift is $+0.56 \pm 0.61\%$, where the uncertainty reflects the expected fluctuations as calculated with the Monte Carlo. In 1994 the values are $+0.56 \pm 0.15\%$ and $+0.06 \pm 0.35\%$, respectively. I calculate the systematic uncertainty on the lifetime associated with the simulation of bremsstrahlung as follows: $1.5 \times 0.82\% \times (0.1266 - 0.1150)/0.1266 = 0.11\%$. Thanks to `tslt02`, the electron fraction before the bremsstrahlung cut is correctly simulated (unlike in past years). The discrepancy in the efficiency of the bremsstrahlung cut is therefore not caused by a discrepancy in the number of electrons entering the cut.

The VDET hit requirement is another cut that rejects bremsstrahlung. I use Bhabha events to study the behavior of the VDET hit association in data and Monte Carlo. The events are selected by requiring exactly one track in each hemisphere (opposite charges) with at least eight TPC hits, $|\cos\theta| < 0.9$, and $p > 1\,\mathrm{GeV}/c$. One hemisphere is chosen at random as a possible tag hemisphere. Events are accepted if the tag track is a high-quality electron with energy near the beam energy. I then plot the momenta and impact parameter of the nearly-unbiased track in the other hemisphere, with various cuts on ITC and VDET hits, helix fit χ^2, and the usual bremsstrahlung rejection. Figure 14a shows the momentum distributions in data and Monte Carlo when no VDET hits are required; the agreement is quite good, indicating that the overall bremsstrahlung rate is accurately simulated. Figures 14b, c, and d show the distributions after the VDET hit and χ^2 cuts are imposed, for the three different configurations of VDET r-ϕ hits. These plots are sensitive to the VDET hit association parameters, and the Monte Carlo reproduces the data fairly well; plot d contains particularly interesting structure. Figures 14e, f, and g

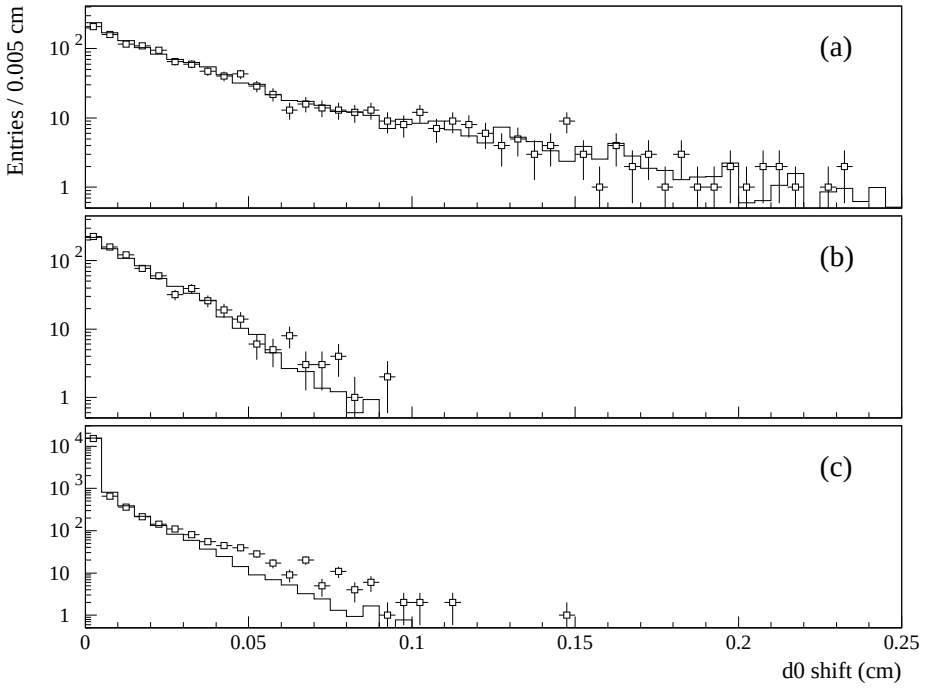

Figure 13. Distribution of the estimated impact parameter shift $|\Delta d_0|$ calculated from ECAL information by the bremsstrahlung rejection program, for 1993 and 1994 data (squares with error bars) and Monte Carlo (histograms): (a) separated γ and e showers; (b) partially merged but separable showers; (c) merged γ and e showers, or electrons with no evidence of bremsstrahlung. The cut removes electron candidates with $|\Delta d_0| > 0.01$ cm. The events plotted here are those that survive all cuts through the track momentum cut and do not contain a track in an exclusion zone.

are the corresponding distributions after the hard bremsstrahlung cut is applied as in the lifetime analysis. Again there is no indication of a deficiency in the simulation.

Figure 15 shows the distribution of $q \times$ (impact parameter sum) for the same seven subsamples of tracks as in fig. 14. This quantity should be near zero for well-measured tracks and positive for tracks that lose energy in the detector material. The impact parameter sum is used in order to reduce the smearing related to the size of the luminous region. The positive tails in data and Monte Carlo agree in the first four plots. There may be some discrepancies after the bremsstrahlung cut is applied (the bottom three plots), but such problems are covered by the analysis of fig. 13 discussed above.

The entries below -0.04 in fig. 15a are very interesting. They are produced by two mechanisms:

- The sense and field wires of the ITC are arranged in radial rows. Tracks passing near one of these rows have a higher probability of being mismeasured, and the Monte Carlo may be underestimating the size of the effect, which is also observed in dimuons. Further studies are planned.

- Some tracks have one or two TPC hits that are wildly mismeasured. When a hit

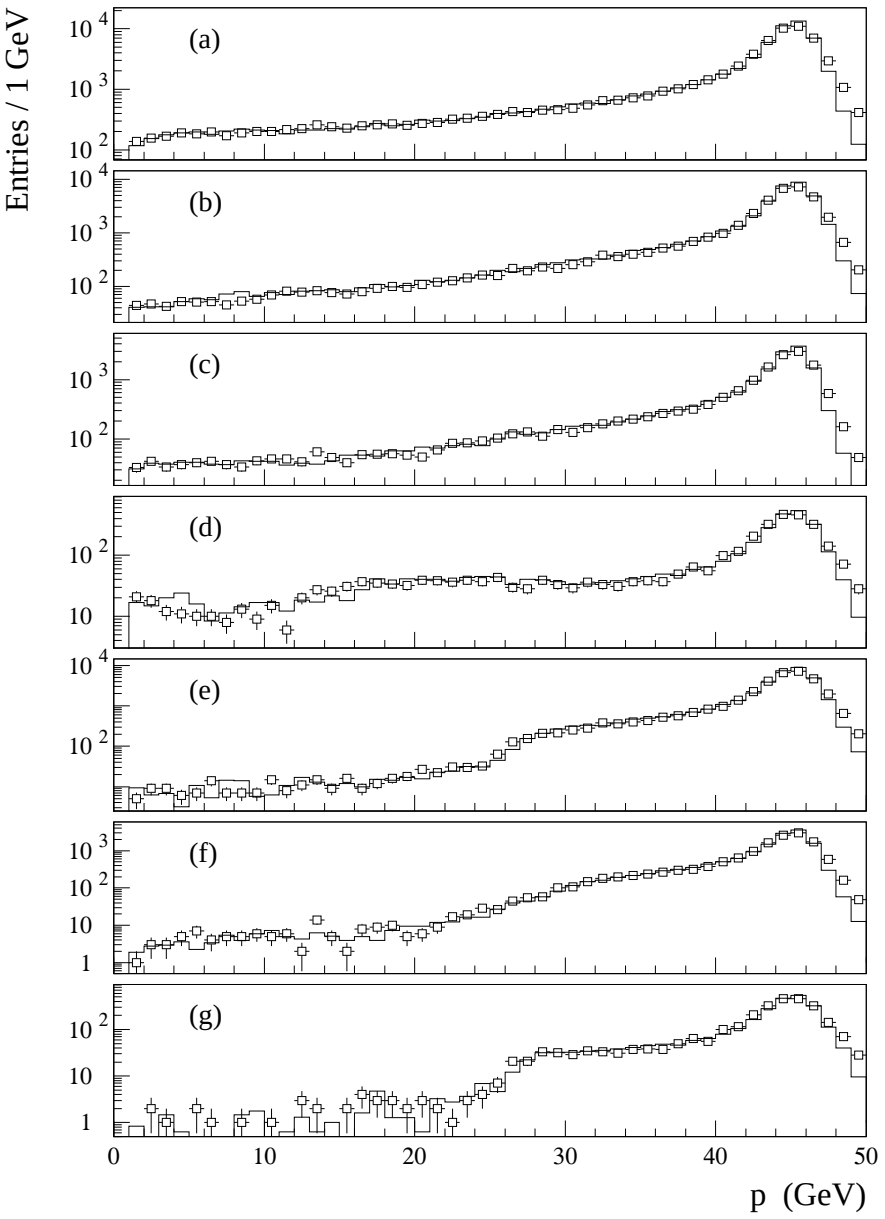

Figure 14. Momenta of electron candidates in Bhabha events in 1993 and 1994 data (squares with error bars) and Monte Carlo (histograms): (a) electrons with at least four ITC hits; (b-d) further requiring $\chi^2/\mathrm{dof} < 5$ and VDET r-ϕ hits in both layers, inner layer only, and outer layer only, respectively; (e-g) same three plots, but further requiring the electrons to pass the hard bremsstrahlung rejection cut. A discrepancy above $45\,\mathrm{GeV}/c$ is present because no off-peak Bhabha Monte Carlo is available for 1993. I used the peak events and scaled the normalizations of all Monte Carlo plots by a common factor such that the data and Monte Carlo in (a) have equal areas. Dimuon and $\tau^+\tau^-$ backgrounds are taken into account in the Monte Carlo plots. The exclusion zones are not used in this Bhabha analysis.

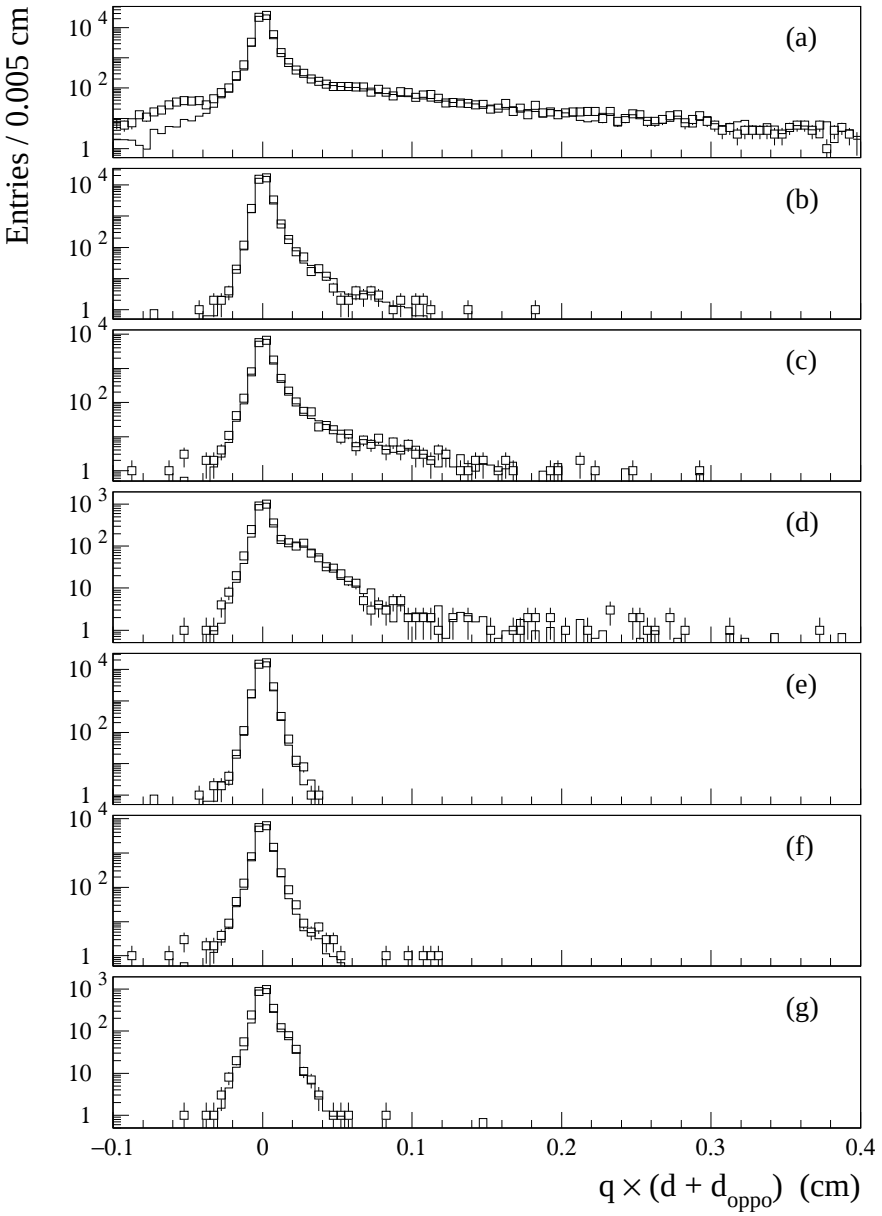

Figure 15. Charge times impact parameter sum for the tracks in the Bhabha events of fig. 14. Bremsstrahlung shifts this quantity toward positive values.

Table 5. Change (in percent) of slope a_1 in Monte Carlo, with respect to the standard conditions, for various cuts on the numbers of generated nucleons per event ($n_{\rm N}$) and extra reconstructed tracks per hemisphere ($n_{\rm extra}$). The first row represents the standard cuts.

	Change in bias (%)	
Cuts	1993	1994
$n_{\rm extra} \leq 2$, no cut on $n_{\rm N}$	0	0
$n_{\rm extra} \leq 2$, $n_{\rm N} = 0$	-0.01 ± 0.02	0.00 ± 0.02
$n_{\rm extra} = 0$, $n_{\rm N} = 0$	-0.14 ± 0.22	-0.17 ± 0.18
no cut on $n_{\rm extra}$ or $n_{\rm N}$	-0.02 ± 0.09	-0.01 ± 0.09

near the outer wall of the TPC is mismeasured, the fitted track can be pulled so badly that the VDET hits are not associated and the measured impact parameter is hundreds of microns off. The track fitter in `julia` does not reject such hits (at least it didn't in these cases), but it should! The effect is greatest for $e^{\pm}$ tracks, suggesting that δ rays are to blame. Another contribution may come from debris splashed out of the ECAL into the last TPC pad row. This phenomenon will also be investigated further. In any case, the Monte Carlo does not correctly simulate the crazy TPC coordinates.

Crazy coordinates are also responsible for the discrepancy between the helix fit χ^2 distributions in data and Monte Carlo. When the crazy hits are not near the inner or outer wall of the TPC, the VDET hits are more likely to be correctly associated with the track. In the past I have shown that the resulting degradation of the d_0 resolution is not significant for tracks with $\chi^2/{\rm dof} < 5$, i.e., those used in the lifetime analysis.

Nuclear interactions. Here I only consider nuclear interactions in which nucleons are ejected from the detector material, because such interactions are explicitly identified in the Monte Carlo truth information. Other kinds of scattering are taken into account by the studies described earlier in this section.

In order to investigate the influence of nuclear interactions on the fitted slope, the data and Monte Carlo are fitted under various cuts. The changes in slope with respect to the standard cuts is given in table 5. An "extra" track is one with $|d_0| < 40\,{\rm cm}$ and at least four TPC hits, but no VDET hits. The first row in the table represents the standard cuts. The second row shows the result of removing all events with nuclear interactions from the Monte Carlo fit; nuclear interactions have a very small effect on the fitted slope. The Monte Carlo accurately predicts the $n_{\rm extra}$ spectrum (fig. 16). I take the systematic uncertainty on the lifetime due to nuclear interactions to be negligible.

Confusion due to extra tracks. A τ daughter track in a one-prong decay may be mismeasured if extra tracks present in the hemisphere cause confusion in the pattern recognition or coordinate measurement. Most of the extra tracks come from photon conversions.

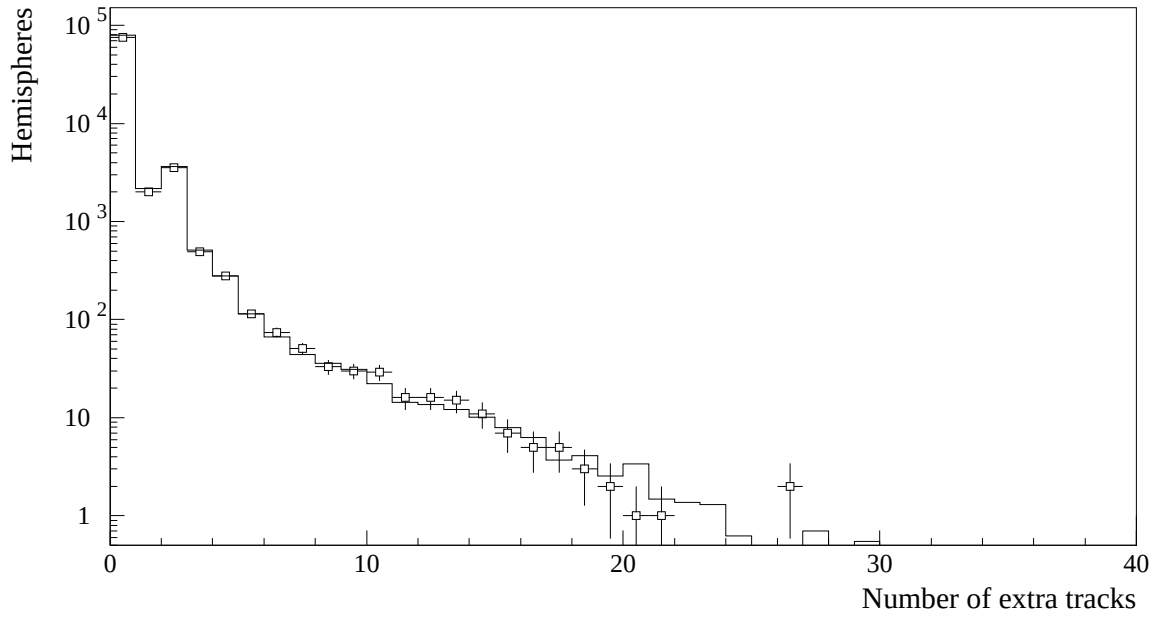

Figure 16. Number of extra tracks per hemisphere, in 1993 and 1994 data (squares with error bars) and Monte Carlo (histogram). The events plotted here are those that survive all cuts through the hard bremsstrahlung cut and do not contain a track in an exclusion zone.

In the 1-1 sample, the fraction of events containing one or two extra tracks is large: $6.43 \pm 0.09\%$ in the data and $6.37 \pm 0.03\%$ in the Monte Carlo (after all cuts). However, because these extra tracks have no VDET hits, the impact parameter measurement of the "good" track is affected in only a small fraction of cases. By comparing the second and third rows of table 5, we see that the effect on the slope of allowing up to two extra tracks per hemisphere (excluding nuclear interactions) is on the order of 0.2%. When the requirement $n_{\rm extra} = 0$ is added to the normal selection, the slope in Monte Carlo (including backgrounds) changes by $-0.16 \pm 0.22\%$ in 1993 and $-0.18 \pm 0.18\%$ in 1994. In data, the corresponding numbers are $-0.46 \pm 0.78\%$ and $-0.55 \pm 0.42\%$. Although the number of events with extra tracks is accurately reproduced by the Monte Carlo, I assign a systematic uncertainty of 0.2% for the simulation of the effect of the extra tracks on the lifetime.

Trimming. Trimming serves to reduce the sensitivity of the measured lifetime to large statistical and possible systematic errors associated with poorly measured daughter tracks. These systematic errors were covered in the preceding discussion. Nevertheless, the trimmed events are not only those that have large errors due to detector resolution: events in which the Z^0 is produced far from the center of the luminous region may also be trimmed, as may events with long-lived τ's.

The bias due to the size of the luminous region was discussed in section 4 in the context of an untrimmed fit, but the systematic errors are still negligible when trimming is applied. The size of the luminous region is measured from the data, and even a 20% error in the size would change the bias due to trimming by less than 0.05%.

It therefore remains to evaluate the systematic uncertainty related to the trimming of long-lived τ's. The issue here is the simulation of the τ decay angles, because events with large decay angles (large $|X|$) tend to have large true impact parameters and hence are more likely to be trimmed away. How important is this effect? If all the trimmed events are restored to the fit with their true values of X and Y (the idealized variables mentioned above, with no errors of any kind), the slope increases by 0.54% in 1993 and 0.34% in 1994. (I don't have the statistical errors, but I believe the difference between the two years is mostly a statistical fluctuation.)

The Monte Carlo lifetimes are rescaled to the measured values as described in section 11 in order to correctly estimate the bias due to trimming of long-lived τ's. The X distribution (fig. 7) is adequately reproduced by the Monte Carlo, so the corresponding systematic error on the lifetime is negligible.

According to Monte Carlo, the trimmed events may be broken down as follows: 64 trimmed events are expected in the combined 1993 and 1994 sample (without "tail enhancement"). Among these, approximately 10 events have long-lived τ's, 50 contain a muon or hadron with a large measurement error (including 10 with nuclear interactions), 3 have an electron with a large measurement error (includes bremsstrahlung), and 1 has a large residual due to the size of the luminous region.

12.9 Backgrounds

The effect of backgrounds on the fitted slope is determined from Monte Carlo. I have considered $e^+e^- \to q\bar{q}$, e^+e^-, and $\mu^+\mu^-$; $\gamma\gamma \to \ell^+\ell^-$ and $q\bar{q}$; and cosmic rays.

A sample of 2.36 million generated $e^+e^- \to q\bar{q}$ events, corresponding to the size of the real data sample, yields no candidate 1-1 events. I estimate the systematic uncertainty by considering one background event with a uniform X distribution over $|X| < 0.18$, and $Y = 0$. The resulting shift in the slope is less than 0.01% and is neglected in the systematic uncertainty on the lifetime.

For the other background channels, I determine the bias on the slope by simply adding appropriately normalized samples of background events to the $\tau^+\tau^-$ Monte Carlo. The observed shifts in the fitted slope are given in table 4. I include a 25% systematic uncertainty for each channel; which amounts to 0.07% in 1993 and 0.05% in 1994.

The background fractions in 1993 within $|X| < 0.18$ are predicted to be 0.08% of $e^+e^- \to e^+e^-$, 0.03% of $e^+e^- \to \mu^+\mu^-$, and 0.33% of $\gamma\gamma \to \ell^+\ell^-$; in 1994 the corresponding numbers are 0.06%, 0.02%, and 0.24%. Figure 17 shows the expected combined Y vs. X distribution for these channels in 1993 and 1994.

I evaluate the contamination due to cosmic rays by selecting events with $|X| < 0.01$ and $0.3 < |Y| < 2\,\mathrm{cm}$. There are three such events. Two of them contain no muons and the daughter tracks have unequal momenta. The third (run 22932 event 9824) looks just like a cosmic ray. The corresponding contamination in the full sample is less than 0.01%.

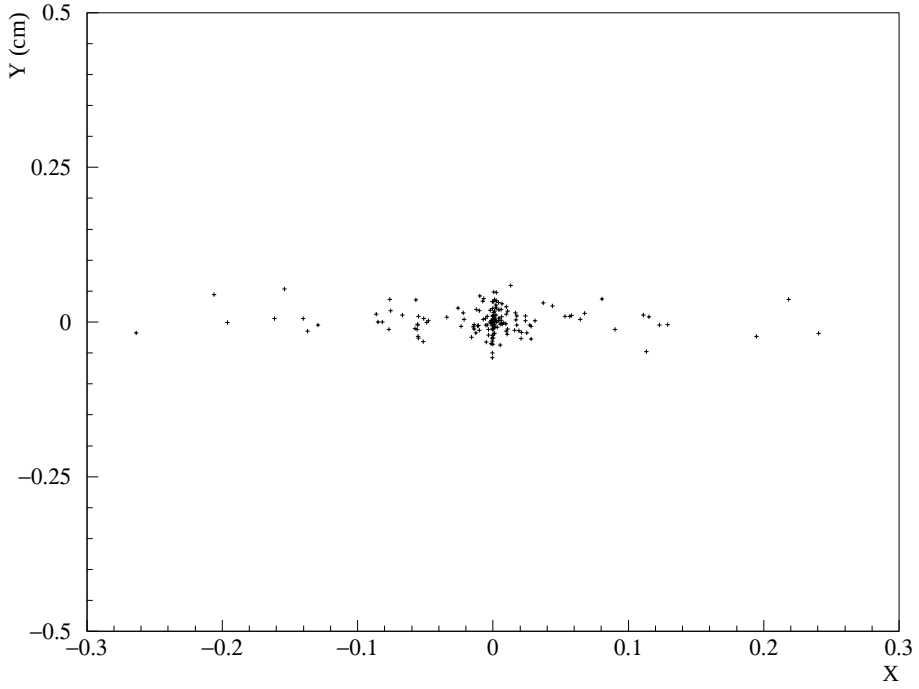

Figure 17. Y vs. X from simulated $Z^0 \to e^+e^-$, $Z^0 \to \mu^+\mu^-$, and $\gamma\gamma \to \ell^+\ell^-$ events. The number of simulated events corresponds to the size of the real 1993 and 1994 data sample.

12.10 Other systematic uncertainties

Other possible sources of systematic error are considered, as in [3]:

- τ branching fractions;
- three-prong τ decays in the 1-1 sample;
- τ mass;
- average τ momentum;
- systematic errors in the $\sin\theta_{\rm thrust}$ determination;
- dimensions of tracking detectors;
- VDET r-ϕ strip pitch;
- track curvature in the magnetic field;
- offset between beam axis positions in data and Monte Carlo.

The resulting uncertainties on the lifetime are found to be negligible.

The fit range in X is varied to check for systematic effects. The limit on $|X|$ (denoted $X_{\rm max}$) is changed from 0.1 to 0.26 in both data and Monte Carlo, and the variations

in the fitted slope are compared. This is done separately for 1993 and 1994. In both years the largest disagreement between data and Monte Carlo occurs for $X_{\max} = 0.26$. However, the discrepancies (data minus Monte Carlo) have opposite signs in the two years: $+0.73 \pm 0.35\%$ in 1993 and $-0.28 \pm 0.20\%$ in 1994, where the uncertainties shown are rather approximate statistical uncertainties determined from Monte Carlo events. (The "tail enhancement" is modified to generate events beyond $|X| = 0.18$ for this test.) Because the 1993 and 1994 data give opposite variations, and the agreement between data and Monte Carlo is satisfactory for $X_{\max} < 0.18$, I am inclined to interpret the discrepancy as a statistical fluctuation. The effect is too large to be related to the simulation of background. (There would need to be much less than zero background in the data to explain the discrepancy.) The only other possible systematic difference between the 1993 and 1994 data that could be relevant here is tracking resolution, which is dealt with in section 12.8.

13 Determination of the Lifetime

The sum of the systematic biases on the slope in 1993 is $-0.58 \pm 0.27 \pm 0.34_{\rm corr}\%$. The corrected value of a_1 is obtained by dividing the fitted value by $(1 - 0.0058)$, yielding

$$a_1 = 0.22115 \pm 0.00482 \pm 0.00059 \pm 0.00075_{\rm corr}\,{\rm cm}.$$

Using $\bar{p}^0_\tau = 45.397\,{\rm GeV}/c$ and $M_\tau = 1.77700\,{\rm GeV}/c^2$ [12], I obtain the result

$$\tau_\tau^{1993} = 288.8 \pm 6.3 \pm 1.3\,{\rm fs}.$$

The statistical uncertainty is calculated in section 11.

In 1994 the net bias is $-0.19 \pm 0.25 \pm 0.42_{\rm corr}\%$, the corrected slope is

$$a_1 = 0.22287 \pm 0.00281 \pm 0.00056 \pm 0.00093_{\rm corr}\,{\rm cm},$$

and the derived lifetime is

$$\tau_\tau^{1994} = 291.0 \pm 3.7 \pm 1.4\,{\rm fs}.$$

The results from 1993 and 1994 are combined by means of our usual procedure [13] to yield the final IPD measurement:

$$\tau_\tau = 290.4 \pm 3.2 \pm 1.3\,{\rm fs},$$

with $\chi^2 = 0.093$ for one degree of freedom. The corresponding confidence level is 0.76.

14 Compared to the preliminary results, what has changed?

An earlier version of this analysis was described by Joe Rothberg in the Thursday Meeting of 14 March 1996. The preliminary result, first presented in public at Moriond in March 1996, was

$$\tau_\tau = 290.4 \pm 3.2 \pm 1.7\,{\rm fs}.$$

The most important improvements made since then are

- New Monte Carlo samples (section 3) are used for signal and backgrounds. (Monte Carlo statistics contributed the largest systematic error in the preliminary analysis.)
- The Pisa d_0 resolution scheme (section 7) was introduced in the calculation of the event weights.
- The dependence of the measured lifetime on $\Delta_{\rm trim}$ was understood and a remedy applied to the Monte Carlo (section 12.8).
- The discrepancy between the helix fit χ^2 distributions in data and Monte Carlo was understood (section 12.8).

Acknowledgements

I would like to thank several people who provided assistance with this analysis: John Putz performed tests of the 1-1 event selection routine and studied d_0 resolution in dimuons. Alberto Lusiani provided d_0 resolution parameters for Monte Carlo and data. Joe Rothberg presented my preliminary results in a Thursday Meeting. Dave Casper, Alain Bonissent, and Raymond Beuselinck responded to my questions about tracking simulation and reconstruction.

References

[1] S. Wasserbaech, ALEPH 91-140 PHYSIC 91-123.

[2] S. Wasserbaech, ALEPH 92-073 PHYSIC 92-064.

[3] S. Wasserbaech, ALEPH 95-026 PHYSIC 95-024.

[4] D. Decamp *et al.*, Phys. Lett. B **279** (1992) 411.

[5] D. Buskulic *et al.*, Phys. Lett. B **297** (1992) 432.

[6] D. Buskulic *et al.*, Z. Phys. C **70** (1996) 549.

[7] D. Buskulic *et al.*, CERN-PPE/97-016 (1997), submitted to Z. Phys. C.

[8] A. Lusiani, talk in the τ meeting, CERN, 23 May 1995.

[9] F. Fidecaro *et al.*, ALEPH 94-115 PHYSIC 94-100.

[10] J. Putz, ALEPH 96-097 PHYSIC 96-089.

[11] H. Videau, talk in the Thursday meeting, CERN, 18 July 1996.

[12] R.M. Barnett et al. (Particle Data Group), Phys. Rev. D **54** (1996) 1.

[13] L. Lyons, D. Gibaut, and P. Clifford, Nucl. Instrum. Methods A **270** (1988) 110.